Identifying new phosphorylation substrates of a viral protein kinase encoded by Kaposi's sarcoma-associated herpesvirus

Sydney DiDonato

The Damania Lab

Department of Microbiology and Immunology

Abstract

Kaposi's sarcoma-associated herpesvirus (KSHV), also known as human herpesvirus 8 (HHV8), is the infectious cause of three types of human cancer: Kaposi's sarcoma, primary effusion lymphoma, and multicentric Castleman's disease. To aid in viral replication, KSHV encodes a viral serine/threonine protein kinase (vPK), a protein that plays a role in the production of infectious KSHV virions. The vPK protein alters the phosphorylation of several cellular substrates, leading to the augmentation of protein synthesis and the multiplication of virally infected cells. While current research shows that vPK can mimic some cellular kinases to phosphorylate approximately ten different cellular substrates, there are likely more substrates for vPK than what is currently known. This project aimed to confirm two new phosphorylation substrates, nucleophosmin (NPM1) and human antigen R (HUR), which were identified by high-throughput phosphoproteomics. Immunoblotting revealed overall protein levels of NPM1 and HUR did not change in the presence or absence of vPK. Additionally, no apparent effect on the phosphorylation of NPM1 by vPK was observed. These results indicate that vPK may not be

affecting the phosphorylation of NPM1. Detection of HUR phosphorylation is still being optimized and it has yet to be determined whether HUR phosphorylation levels are affected in the presence of vPK. The identification of new phosphorylation substrates of vPK, such as NPM1 and HUR, has the potential for the development of new treatments for KSHV-related cancers by targeting vPK kinase activity.

Introduction

Kaposi's sarcoma-associated herpesvirus (KSHV), also known as human herpesvirus 8 (HHV8), is an oncovirus[1]. As a member of the herpesvirus family, KSHV causes lifelong infection in the host[2]. The virus infects endothelial cells, B cells, monocytes, dendritic cells, and epithelial cells[1]. KSHV is the infectious cause of three types of human cancer: Kaposi's sarcoma (KS)[3], primary effusion lymphoma[4], and multicentric Castleman's disease[5]. KS is the most common type of cancer in individuals with HIV/AIDS[6]. While KSHV is necessary for KS development, cofactors are required to activate KSHV out of dormancy and produce sarcoma[1]. The most common cofactor is HIV infection, but other causes of immunodeficiency serve as cofactors for KS development as well[1].

KSHV, like all herpesviruses, is an enveloped, double-stranded DNA virus with two different life cycles: latent and lytic[2]. During primary infection, KSHV encounters multiple components of the innate immune response which induce the virus to establish molecular latency[1]. During latency, the main goal of KSHV is survival[2]. The virus does not replicate during latency but induces the proliferation of infected cells to transfer the viral genome[2]. KSHV encodes several latent proteins that allow the virus to evade the host's innate and adaptive

immune responses, induce cellular proliferation, prevent apoptosis, and change the cellular environment to establish and maintain latency[7].

The process of maintaining latency coincides with many of the hallmarks of cancer[8]. As the virus alters the cellular environment to maintain latency and survive in host cells, KSHV can lead to the formation of cancer[7].

During lytic replication, new virions are made and the virus is transmittable[9]. One of the proteins that the virus expresses during the lytic stage is a viral serine/threonine protein kinase (vPK), which is encoded by the ORF36 gene[10]. vPK plays a role in the production of KSHV virions to aid in the transmission of the virus[11]. As a kinase, vPK adds phosphate groups to cellular proteins through a process called phosphorylation[10]. Protein phosphorylation activates cellular pathways and alters protein interactions, making it an important process for cellular events such as signal transduction, cell growth, and protein synthesis[12]. vPK alters the phosphorylation of host proteins, leading to the activation of protein synthesis and the multiplication of virally infected cells[13]. Expression of vPK can also induce angiogenesis, which causes the formation of new blood vessels to supply KSHV-infected cancer cells with nutrients to survive[13].

Based on current research, vPK seems to be mimicking several cellular kinases. To aid in viral replication, vPK acts like cyclin-dependent kinase 2 (CDK2)[14], one of the CDKs that plays a vital role in cell cycle regulation[15]. vPK also mimics the function of cellular S6 kinase B1 (S6KB1), a protein with target substrates involved in protein synthesis, cellular proliferation, and vascularization[13]. vPK has the ability to bypass the regulation of upstream kinases in the S6 pathway that would otherwise inhibit protein synthesis during viral infection to activate S6[12]. In

addition to CDK2 and S6KB1 substrates, vPK phosphorylates several other cellular substrates including eukaryotic initiation factor 4E (eIF4E)[12] and c-Jun N-terminal kinase (JNK)[16].

Our lab hypothesizes that there are still more vPK substrates than what is currently known. In order to characterize novel phosphorylation substrates of vPK, cells were collected by the Damania Lab and submitted to the Proteomics Core at the University of North Carolina at Chapel Hill. The following work uses immunoblotting and immunoprecipitation experiments in an attempt to confirm two of the phosphorylation substrates identified by high-throughput phosphoproteomics. For one of these substrates, no effect on phosphorylation was observed in the presence of vPK. It has yet to be determined whether phosphorylation levels of the second substrate are affected in the presence of vPK. The continuation of this project to study how vPK affects the activity of these proteins and others will allow for a greater understanding of how viral proteins alter the cellular environment, with the potential for the development of new treatments for KSHV-related cancers that target vPK kinase activity.

Materials and Method

Cell Culture. Cells from the malignant human B-cell line (BJAB), human embryonic kidney-293T (HEK-293T) cells, and human umbilical vein endothelial cells (HUVECs) were used. BJAB cells were previously transduced by my postdoctoral mentor, Dr. Ariana Bravo Cruz, to stably express empty vector (EV) or vPK. These cells were grown in RPMI media supplemented with 10% fetal bovine serum (FBS), penicillin and streptomycin (100 U/µl), 2mM L-glutamine and maintained under geneticin selection (0.8 ml/ml). HEK-293T cells were grown in D-MEM media supplemented with 10% FBS, penicillin and streptomycin (100 U/µl), and 2mM L-glutamine. HUVECs were previously transduced to stably express EV or vPK[12] and were grown

in endothelial cell growth media with 10% FBS, as described above. Cells were kept in an incubator at 37^0C with 5% CO_2.

Transfections. HEK-293T cells were plated in 6-well plates (5×10^5 cells per well) for 24 hours and then transfected using Lipofectamine 3000 Reagent with 2,000 µg of an EV or vector-expressing v5-tagged vPK protein, previously generated by the Damania lab, for an additional 24 hours.

Cell conditioning. For serum starvation, transfected HEK-293T or transduced BJAB cells were incubated in fresh media with 10% FBS (normal conditions) or in media without FBS (starvation conditions) for 24 hours. To synchronize cells in G2/M phase, HUVECs were plated in 10 cm dishes with 10% FBS for 24 hours and then incubated in 5% FBS with 100 µg/mL InSolution™ Nocodazole (Sigma-Aldrich) for 16 hours.

Immunoblots. BJAB EV and BJAB vPK-expressing cells were collected by centrifugation at 1500 RPM for 3 minutes and the supernatant was removed. Cells were lysed using NP-40 buffer (1% NP-40, 50 mM Tris-HCl pH 8, 150 mM NaCl, protease inhibitor tablet, 30 mM beta-glycerolphosphate, 50 mM NaF, 1 mM Na3VO4), then incubated on ice for 15 minutes. Lysates were centrifuged at 13,200 rpm for 10 minutes. While BJABs were grown in suspension, HEK-293T cells and HUVECS are adherent cell lines and required different conditions for lysate collection. Lysates of HEK-293T cells and HUVECs were generated as described below. D-MEM or endothelial cell growth media was aspirated from each well and cells were washed with ice-cold PBS. PBS was aspirated and cells were lysed with NP-40 buffer. Lysates were

transferred to Eppendorf tubes and incubated on ice for 15 minutes, then centrifuged at 13,200 rpm for 10 minutes.

Protein concentrations were calculated using the Bradford technique. Equal amounts of proteins were electrophoresed on 12.5% sodium dodecyl sulfate-polyacrylamide gel electrophoresis (SDS-PAGE), with the exception of an 8% SDS-PAGE gel used for the immunoblot in Figure 1A. Transfer onto nitrocellulose membrane followed. Membranes were blocked for 30 minutes at room temperature with milk or BSA depending on the manufacturer's recommendations for the antibodies, then incubated overnight at 4°C with the appropriate primary antibody. The following primary antibodies were used: anti-vPK (1:500, generated by Genescript using a GST-tagged 1-150 amino acid vPK fragment); anti-v5-HRP (1:1000, Invitrogen, 46-0708); anti-HUR (1:1000, Santa Cruz Biotechnology, sc-5261); anti-nucleophosmin (1:2500, Abcam, ab10530); anti-phospho nucleophosmin (Thr234/237, 1:1000, Abcam, ab118637); anti-eIF4E (1:1660, Cell Signaling Technology, 2067S); anti-phospho eIF4E (1:1660, Cell Signaling Technology, 9741S); anti-tubulin (1:5000, Cell Signaling Technology, 9099S); anti-phosphoserine CDK substrate (1:1000, Cell Signaling Technology, 9477S); anti-phospho CDC2 (1:1000, Cell Signaling Technology, 9114S); anti-tubulin (1:5000, Cell Signaling Technology, 9099S); anti-mouse IgG HRP (1:1000, eBioscience E07429-1634).

After washing with TBS-T to remove unbound antibodies, membranes were incubated with the appropriate HRP-conjugated secondary antibody for one hour at room temperature: anti-mouse IgG (1: 2000, Cell Signaling Technology, 7076S) or anti-rabbit IgG (1:2000, Cell Signaling Technology, 7074S). Results were visualized with the Bio-Rad Clarity Western Blotting Detection System. Bands were visualized using chemiluminescence imaging.

Immunoprecipitations. HEK-293T cells, BJAB cells, and HUVECs lysates were collected as described above. Protein concentrations were calculated using the Bradford technique. For HUR and IgG immunoprecipitations, samples were prepared with 200 µg of lysate, 1 µg of antibody, and various amounts of NP-40 buffer to bring the total volume of each sample to 1 mL. For vPK immunoprecipitations, samples were prepared with 200 µg of lysate, 2.5 µg of antibody, and various amounts of NP-40 buffer to bring the total volume of the sample to 1 mL. Samples were incubated at 4°C for 2 hours. At 2 hours, 20 µL of Protein A/G PLUS-Agarose Immunoprecipitation Reagent (Santa Cruz Biotechnology, sc-2003) was added to each sample. Samples were then incubated at 4°C overnight. The following day, samples were centrifuged at 8,000 rpm for 30 seconds. After centrifugation, the supernatant was aspirated and the pellet was washed with 1 mL of NP-40 buffer followed by centrifugation. Samples were washed for a total of 4 times and then boiled at 95°C for 10 minutes with 40 µL of laemmli sample buffer. Samples were centrifuged at 8,000 rpm once more following denaturation. Immunoblotting followed.

Results

NPM1 and HUR were identified as potential vPK substrates. To identify potential novel phosphorylation substrates of vPK, cell lysates from EV or vPK-expressing BJAB cells and HUVECs were collected by Dr. Ariana Bravo Cruz and submitted to the Proteomics Core at the University of North Carolina at Chapel Hill. The samples were analyzed by the Proteomics Core and a phosphoproteomic data set was generated, providing a list of human substrates that are likely to be phosphorylation targets of vPK, hereafter referred to as hits. Two hits from the high-throughput phosphoproteomic data were of particular interest, NPM1 and HUR. The *NPM1* gene

encodes a phosphoprotein called nucleophosmin, which affects chromatin remodeling, embryogenesis, and genome stability[17]. The disrupted regulation of NPM1 phosphorylation can result in a dysregulated cell cycle and cancer formation[15]. The *HUR* gene encodes human antigen R, an RNA-binding protein that is known to increase the stability of mRNAs, including a number of cancer-related mRNAs[18]. The expression of *HUR* is also linked to tumorigenesis and the formation of multiple types of cancer[16]. Interestingly, NPM1 and HUR are both substrates of cyclin-dependent kinases (CDKs)[15-16], a type of kinase that vPK is known to share functional similarities with[14]. The identification of NPM1, HUR, and several other proteins as high-throughput phosphorylation substrates of vPK indicated that vPK is likely phosphorylating more cellular substrates than what is currently known.

A new anti-vPK antibody is suitable for immunoblotting and immunoprecipitations. In order to characterize the novel phosphorylation targets of vPK, the conditions for a new anti-vPK antibody first had to be optimized. This antibody was necessary to confirm the expression of vPK in cells that were transfected (HEK-293T cells) or transduced (BJAB cells and HUVECs), but was recently acquired by the Damania Lab and had never before been used. Lysates from BJAB cells stably expressing EV or vPK were collected and immunoblotting was performed with the new anti-vPK antibody. Conditions for this antibody were optimized using another anti-vPK antibody as a positive control. The positive control anti-vPK antibody had been readily used in the Damania Lab, although a limited quantity remained as it was a gift from another lab. With both antibodies, vPK was detected at approximately 50 kDa in vPK-expressing BJAB samples (Figure 1A); vPK is known to have a molecular weight (MW) of approximately 50 kDa. With

the new anti-vPK antibody, there was a non-specific band that appeared above the vPK band in both EV and vPK-expressing samples, above 50 kDa (Figure 1A). The 50 kDa vPK band is indicated by an arrow (Figure 1A). While expression of vPK was detectable using the new anti-vPK antibody, the dilution required was higher than the dilution required of the gifted anti-vPK antibody (1:500 compared to 1:10,000). In addition to the 1:500 dilution factor, 10% milk was determined to be the best blocking condition for the new anti-vPK antibody because it showed less nonspecific binding compared to blots blocked with 5% milk.

In addition to determining if the new anti-vPK antibody was able to detect vPK by immunoblotting, it was also imperative to determine if the new anti-vPK antibody could be used in immunoprecipitation assays to pull down vPK. Immunoprecipitations would be necessary as the project continued to test for the interactions between vPK and potential cellular substrates like NPM1 and HUR. We immunoprecipitated vPK from HEK-293T cell lysates with the new anti-vPK antibody then immunoblotted using an HRP-linked antibody that recognizes the v5 epitope of vPK. We found that the new anti-vPK antibody is suitable for immunoprecipitation assays (Figure 2B). In sum, the new anti-vPK antibody was found to be suitable for both immunoblotting and coimmunoprecipitation assays.

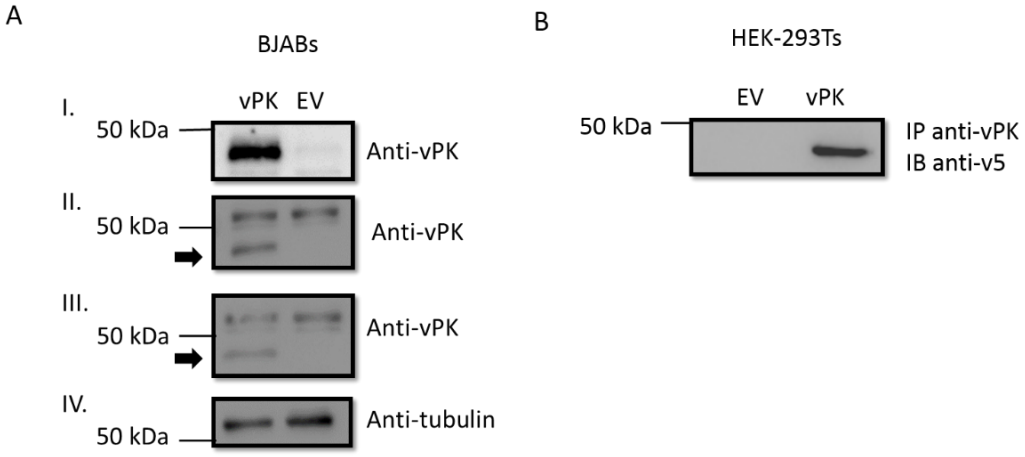

Figure 1. A new anti-vPK antibody is suitable for immunoblotting and immunoprecipitations. (A) Immunoblot of lysates prepared from BJAB cells transduced to stably express EV or vPK. Blots were probed with the gifted anti-vPK antibody as a positive control (I), the new anti-vPK antibody blocked in 5% milk (II), the new anti-vPK antibody blocked in 10% milk (III), or tubulin as a loading control (IV). Arrows in (II) and (III) indicate the vPK band. (B) Immunoblot of lysates prepared HEK-293T cells transfected with either EV or vPK under normal conditions for 24 hours. vPK was immunoprecipitated with the new anti-vPK antibody and blots were probed with an anti-v5 HRP-linked antibody to detect the presence of vPK.

NPM1 phosphorylation appears unaffected by vPK. Phosphoproteomic data revealed that NPM1 phosphorylation was likely to be increased by vPK, but this had not yet been validated by a biochemical assay. To confirm this result, immunoblotting was performed to test for differences in phospho-NPM1 levels between EV and vPK-expressing cells. HEK-293T cells were used because they are an easily transfectable cell line commonly used to study signaling pathways. Serum starvation was performed to synchronize cells to G0/G1 cell cycle phase and reduce basal cellular activity to potentially facilitate the visualization of the phosphorylation state of CDK substrates[19]. Conditions for the anti-phospho NPM1 and anti-NPM1 antibodies were optimized because this was the first time that these antibodies had been used in the Damania Lab. Blots were probed for phospho-NPM1 and total NPM1, which has an expected MW of 32 kDa. In an immunoblot, equal concentrations of NPM1 in EV and vPK-expressing cells should be seen if

vPK solely alters phosphorylation of NPM1 but has no effect on total protein levels. NPM1 levels were consistent among EV and vPK-expressing cells under starvation and normal conditions (Figure 2A). In addition, no differences were observed in phospho-NPM1 levels between EV and vPK-expressing cells under starvation conditions (Figure 2A). However, under normal conditions, there seemed to be a decrease in phospho-NPM1 protein levels in vPK-expressing cells compared to EV-expressing cells (Figure 2A). The same set of blots was also probed with the anti-vPK antibody to confirm vPK expression in the vPK-expressing cells (Figure 2A).

While an increase of NPM1 phosphorylation was not detected in HEK-293T cells, this was not one of the cell lines that was submitted for phosphoproteomic analysis, bringing to our attention the possibility that vPK's kinase activity on NPM1 could be cell type specific. To determine if we could detect differences in NPM1 phosphorylation in one of the cell lines that was used to generate the phosphoproteomic data, immunoblotting was performed with lysates from BJAB cells that were transduced to stably express EV or vPK. Blots were probed for phospho-NPM1, phospho-eIF4e, total eIF4e, tubulin, and vPK. eIF4e is a known substrate of vPK[13] and is shown as a positive control to confirm that vPK kinase activity was functioning (Figure 2B). Blots were probed with the anti-vPK antibody to confirm vPK expression. Tubulin is shown as a loading control (Figure 2B). A slight increase in phospho-eIF4E levels was observed in vPK-expressing cells (Figure 2B). No differences were observed in phospho-NPM1 levels between EV and vPK expressing cells under both starvation and normal conditions (Figure 2B).

Given that no differences in phospho-NPM1 levels were observed in HEK-293T cells or BJAB cells, the specificity of the anti phospho-NPM1 antibody to detect only phosphorylated NPM1 and not total NPM1 was questioned. To confirm that the anti-phospho NPM1 antibody was specific to phospho-NPM1, HUVECs cells were treated with nocodazole. Nocodazole is known to enhance the phosphorylation of CDK substrates, including NPM1, by synchronizing cells to G2/M cell cycle phase, during which CDK1 is active[20]. Hence, nocodazole served here as a positive control. HUVECs were used because previous literature has shown a notable difference in the phosphorylation of HUR, another CDK1 substrate, in HUVECs treated with nocodazole[18]. In addition, HUVECs were included in the phosphoproteomics screen. To confirm that treatment with nocodazole was efficient to induce phosphorylation of CDK's substrates, lysates from HUVECs were immunoblotted with an antibody that recognizes phosphoserine residues only on CDK substrates. Thus, one would expect to see an increase in levels of phosphorylated serine residues on CDK substrates in HUVECs treated with nocodazole. Immunoblotting indeed revealed an increase in the levels of phosphorylated serine residues on CDK substrates in both EV and vPK-expressing cells that were treated with nocodazole (Figure 2C).

Knowing that nocodazole effectively induced phosphorylation of CDK's substrates, the next question addressed was if we could detect an increase in NPM1 phosphorylation in cells treated with nocodazole, which would confirm the specificity of the anti-phospho NPM1 antibody to detect only phosphorylated NPM1 and not total NPM1. Immunoblotting revealed an increase of phospho-NPM1 in EV lysates treated with nocodazole in comparison to untreated EV lysates, suggesting that nocodazole successfully enhanced the phosphorylation of NPM1 (Figure 2D) and that the anti-phospho NPM1 antibody is specific, given that total NPM1 levels were

consistent among the nocodazole-treated and untreated cells (Figure 2D). If NPM1 was phosphorylated by vPK, one would expect to see an increase in the concentration of phospho-NPM1 in vPK-expressing HUVECs. However, phospho-NPM1 levels were consistent between the EV and vPK-expressing cells in both nocodazole treated and untreated cells (Figure 2D). Together, these results demonstrate no increase in phospho-NPM1 levels in vPK-expressing cells across three different cell types (Figure 2).

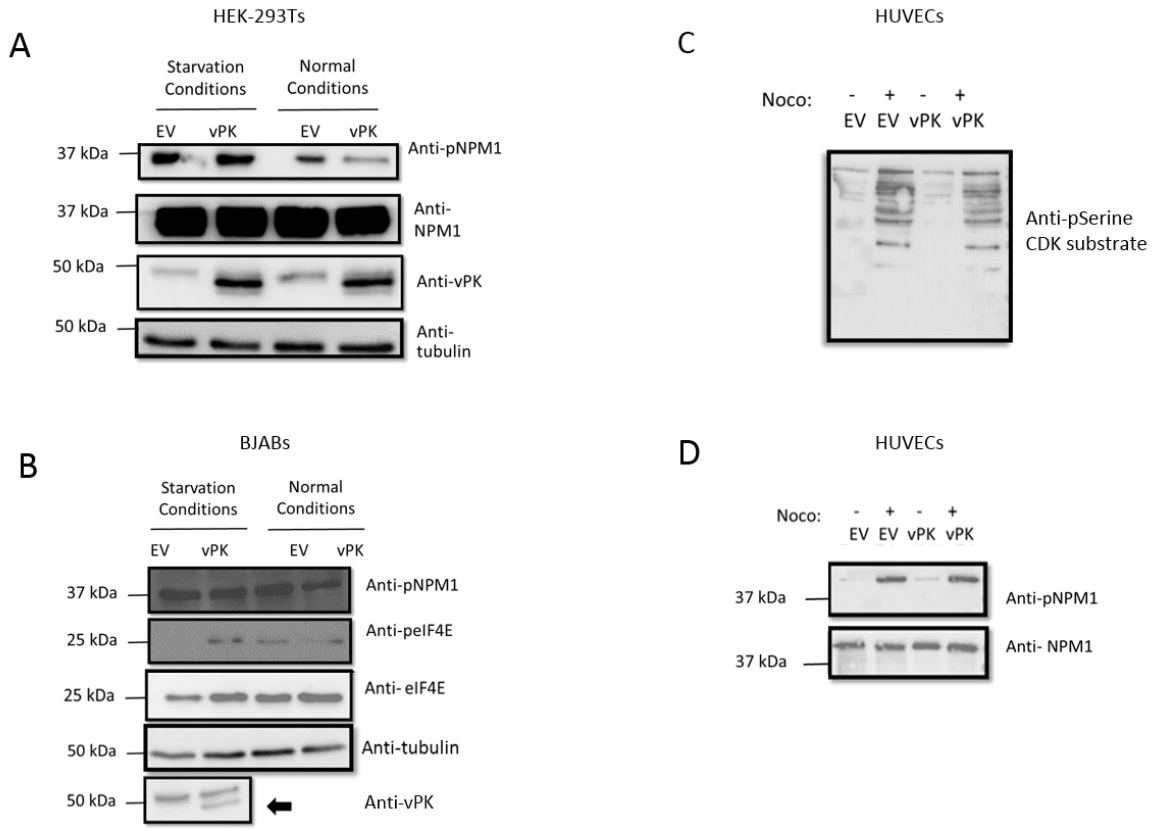

Figure 2. NPM1 phosphorylation appears unaffected by vPK. (A) Immunoblot analysis of lysates prepared from HEK-293T cells transfected with EV or vPK under starvation conditions or normal conditions for 24 hours. Blots were probed with the indicated antibodies. (B) Immunoblot analysis of lysates prepared from BJABs cells transduced to stably express EV or vPK under starvation or normal conditions for 24 hours. Blots were probed with the indicated antibodies. The arrow indicates the vPK band in the last panel. (C) Immunoblot analysis of lysates prepared from HUVECs transduced to stably express EV or vPK and treated with (+) or without (-) nocodazole in 5% FBS for 16 hours. Blots were probed with the indicated antibodies. Representative of two replicates. (D) Immunoblot analysis of lysates prepared from HUVECs transduced to stably express EV or vPK and treated with

(+) nocodazole in 5% FBS for 16 hours or left untreated (-). Blots were probed with the indicated antibodies. Representative of two replicates.

HUR does not appear to be interacting with vPK. Similarly to NPM1, it needed to be determined whether vPK was truly affecting the phosphorylation of HUR. If vPK does alter the phosphorylation of HUR, there should be a difference in levels of phosphorylated HUR protein between EV and vPK-expressing cells and no difference in total HUR protein levels. To confirm that there was no difference in total HUR protein levels among EV and vPK-expressing cells, immunoblotting was performed with HEK-293T cells. As before, HEK 293T cells were used because they are an easily transfectable cell line that is commonly used to study cell signaling pathways. Blots were probed for HUR, which has an expected MW of 36 kDa, using the same lysates from Figure 2. HUR was detected at a consistent level among EV and vPK-expressing cells (Figure 3A).

One indication that HUR is a vPK phosphorylation substrate is a detectable interaction between vPK and HUR. In order to test for any interaction between vPK and HUR, coimmunoprecipitations were performed by incubating BJAB lysates with an anti-HUR antibody to pull down HUR, followed by immunoblotting with an anti-vPK antibody. vPK was not observed in the immunoblots, suggesting no interaction between vPK and HUR (Figure 3B, upper panel). Lysates immunoblotted with anti-HUR antibody showed that HUR was successfully pulled down in all samples (Figure 3B, middle panel). Immunoprecipitation with an anti-IgG antibody was performed to ensure specificity of the antibodies utilized for pulldowns (Figure 3B, lower panel).

Based on the results from the coimmunoprecipitations, it seemed that vPK and HUR were not interacting. However, vPK could have the function of phosphorylating HUR without interacting with it directly. Knowing that an increase in levels of phosphoserine CDK substrates could be visualized after treating cells with nocodazole (Figure 2C), the next question addressed was if we could detect a difference in HUR phosphorylation in nocodazole-treated cells and further enhanced phosphorylation in vPK-expressing cells. Immunoprecipitation assays were performed as there are no readily available antibodies to detect HUR phosphorylated at serine 202, which was predicted by phosphoproteomics to be the residue phosphorylated by vPK. Total HUR protein was immunoprecipitated from EV and vPK-expressing HUVECs samples that were either treated with nocodazole for 16 hours or left untreated. To ensure that the bands being visualized were not the result of non-specific binding, immunoprecipitation assays were also performed with anti-mouse IgG antibody, which should not have been able to pull down the protein of interest. HUR was not detected at the expected MW of 36 kDa with the anti-phosphoserine CDK substrate antibody (Figure 3C), even in samples treated with nocodazole. Blots probed for phosphoserine CDK substrates also showed a significant amount of nonspecific binding (Figure 3C). HUR was detected at 36 kDa in the samples immunoprecipitated with anti-HUR antibody, followed by immunoblotting with anti-HUR antibody, meaning that HUR pulldown was successful (Figure 3C). The 36 kDa band is not present in the immunoprecipitated IgG sample, which is the expected result from the negative control and indicates that the 36 kDa band in the aforementioned blot was not a result of nonspecific binding (Figure 3C). Despite the successful pulldown of HUR, vPK was not detected in the coimmunoprecipitation assay with HUR (Figure 3C), as is also shown in Figure 3B. As a whole, these findings show no apparent

interaction between vPK and HUR and the inability to detect phosphorylated HUR, even in samples treated with nocodazole (Figure 3).

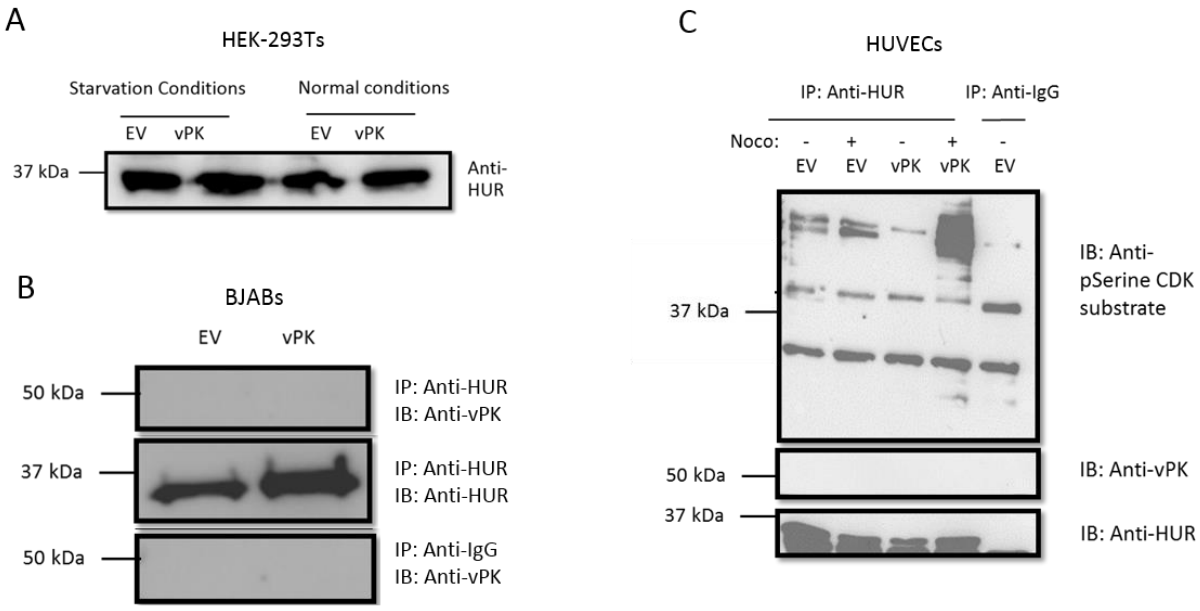

Figure 3. HUR does not appear to be interacting with vPK. (A) Immunoblot analysis of lysates prepared from HEK-293T cells transfected with either EV or vPK under starvation conditions or normal conditions for 24 hours. Blots were probed with the indicated antibodies. (B) Immunoblot analysis of lysates prepared from BJABs cells transduced to stably express EV or vPK under normal conditions for 24 hours. Immunoprecipitations were performed as indicated. Blots were probed with the indicated antibodies. (C) Immunoblot analysis of lysates prepared from HUVECs transduced to stably express EV or vPK and treated with (+) nocodazole in 5% FBS for 16 hours or left untreated (-). Immunoprecipitations were performed as indicated. Blots were probed with the indicated antibodies.

Discussion

Immunoblotting revealed that the overall protein levels of two cellular substrates of interest, NPM1 and HUR, were not changed in the presence or absence of vPK (Figure 2-3). It was expected that vPK would not affect the total concentrations of these proteins if vPK functioned strictly to phosphorylate these substrates, which was confirmed. However, NPM1 phosphorylation was not increased in vPK-expressing cells (Figure 2). Coimmunoprecipitations

indicated that vPK may not be interacting with HUR (Figure 3), despite phosphoproteomic data suggesting that HUR is a likely phosphorylation target of vPK.

From our results, we can infer that NPM1 phosphorylation is not affected by vPK. It can also be inferred that vPK and HUR do not interact, however, this experiment should be repeated with better controls. Whether or not vPK phosphorylates HUR remains elusive. More immunoprecipitation experiments will be performed to determine if vPK affects the phosphorylation status of HUR. If it is determined that vPK is able to phosphorylate HUR, further research will be done to determine if vPK directly phosphorylates HUR or an upstream regulator. While it seems unlikely that NPM1 is a substrate of vPK, other high-throughput cellular substrates from the phosphoproteomic data could still be investigated. One potential substrate of vPK that we are starting to explore is Ras-related protein 1 (Rab1).

One caveat of immunoprecipitations is that the binding sites for either the vPK or HUR antibodies might be masked by an interaction between vPK and HUR. To address this, we can instead perform coimmunoprecipitations with antibodies against tagged vPK and HUR proteins. Another caveat of immunoprecipitations is the amount of nonspecific binding, which can be seen especially in Figure 3D. This can be addressed in the future by adding a "pre-clearing" step to the immunoprecipitation protocol, which would significantly reduce the amount of nonspecific binding.

It was unexpected that we would experience difficulty detecting an increase in phospho-eIF4E levels in vPK-expressing cells (Figure 2B), which disagrees with literature that shows eIF4E as a substrate of vPK[13]. Immunoblotting was also performed for phospho-S6, another known substrate of vPK[13], but an increase in S6 phosphorylation could not be detected in vPK-

expressing cells (not shown). A possible interpretation of these findings is that the immunoblotting technique still needs to be optimized for better detection of phosphorylated vPK's substrates. An alternative to immunoblotting could be to test for HUR phosphorylation *in vivo* using radiolabeled ATP[20].

Overall, the identification of new phosphorylation substrates of vPK, such as NPM1 and HUR, has the potential for the development of new treatments for KSHV-related cancers by targeting vPK kinase activity. KSHV is able to establish cancer in its host by manipulating the cellular environment and vPK has been shown to aid in this process by altering protein phosphorylation, which can activate protein synthesis, induce angiogenesis, and promote the multiplication of virally infected cells[18].

Acknowledgments

I gratefully thank Blossom Damania for giving me the opportunity to be a member of this lab. Special thanks to Ariana Bravo Cruz, whom I am indebted to for her coaching, advice, patience, and assistance in preparing this paper. Thank you to Lorrie Cramer for connecting me with the lab. I also thank Ricardo Rivera-Soto for allowing me to use his 95% ethanol regularly, Jason Wong for his advice on antibodies, Guoxin Ni for cells, Danielle Chappell for her help and encouragement with my future career goals, Zhe Ma for the plants that now brighten my room, Whitney Tevebaugh for keeping Slack full of cat pictures, Darin Weed for the constant updates on his new dog, and the entire lab for keeping the food station stocked with snacks, especially on days when I forgot to pack a lunch.

References

1. Dittmer, D. P. & Damania, B. Kaposi sarcoma-associated herpesvirus: immunobiology, oncogenesis, and therapy. *J. Clin. Invest.* **126**, 3165–3175 (2016).

2. Grinde, B. Herpesviruses: latency and reactivation - viral strategies and host response. *J. Oral Microbiol.* **5**, (2013).

3. Moore, P. S. & Chang, Y. Detection of Herpesvirus-Like DNA Sequences in Kaposi's Sarcoma in Patients with and Those without HIV Infection. *N. Engl. J. Med.* **332**, 1181–1185 (1995).

4. Nador, R. G. *et al.* Primary effusion lymphoma: a distinct clinicopathologic entity associated with the Kaposi's sarcoma-associated herpes virus. *Blood* **88**, 645–56 (1996).

5. Soulier, J. *et al.* Kaposi's sarcoma-associated herpesvirus-like DNA sequences in multicentric Castleman's disease. *Blood* **86**, 1276–80 (1995).

6. Silverberg, M. J. *et al.* Cumulative Incidence of Cancer Among Persons With HIV in North America: A Cohort Study. *Ann. Intern. Med.* **163**, 507–18 (2015).

7. Mesri, E. A., Cesarman, E. & Boshoff, C. Kaposi's sarcoma and its associated herpesvirus. *Nat. Rev. Cancer* **10**, 707–19 (2010).

8. Mesri, E. A., Feitelson, M. A. & Munger, K. Human Viral Oncogenesis: A Cancer Hallmarks Analysis. *Cell Host Microbe* **15**, 266–282 (2014).

9. Jenner, R. G., Albà, M. M., Boshoff, C. & Kellam, P. Kaposi's sarcoma-associated herpesvirus latent and lytic gene expression as revealed by DNA arrays. *J. Virol.* **75**, 891–902 (2001).

10. Park, J., Lee, D., Choe, J., Seo, T. & Chung, J. Kaposi's sarcoma-associated herpesvirus (human herpesvirus-8) open reading frame 36 protein is a serine protein kinase. *J. Gen.*

Virol. **81**, 1067–1071 (2000).

11. Avey, D. *et al.* Discovery of a Coregulatory Interaction between Kaposi's Sarcoma-Associated Herpesvirus ORF45 and the Viral Protein Kinase ORF36. *J. Virol.* **90**, 5953–5964 (2016).
12. Ardito, F., Giuliani, M., Perrone, D., Troiano, G. & Lo Muzio, L. The crucial role of protein phosphorylation in cell signaling and its use as targeted therapy (Review). *Int. J. Mol. Med.* **40**, 271–280 (2017).
13. Bhatt, A. P. *et al.* A viral kinase mimics S6 kinase to enhance cell proliferation. *Proc. Natl. Acad. Sci. U. S. A.* **113**, 7876–81 (2016).
14. Izumiya, Y. *et al.* Kaposi's Sarcoma-Associated Herpesvirus-Encoded Protein Kinase and Its Interaction with K-bZIP. *J. Virol.* **81**, 1072–1082 (2007).
15. Malumbres, M. Cyclin-dependent kinases. *Genome Biol.* **15**, 122 (2014).
16. Hamza, M. S. *et al.* ORF36 Protein Kinase of Kaposi's Sarcoma Herpesvirus Activates the c-Jun N-terminal Kinase Signaling Pathway. *J. Biol. Chem.* **279**, 38325–38330 (2004).
17. Boucher, D. *et al.* Nucleophosmin: from structure and function to disease development. *BMC Mol. Biol.* **17**, 19 (2016).
18. Wang, J. *et al.* Multiple Functions of the RNA-Binding Protein HuR in Cancer Progression, Treatment Responses and Prognosis. *Int. J. Mol. Sci.* **14**, 10015–10041 (2013).
19. Aghababazadeh, M. & Kerachian, M. A. Cell fasting: Cellular response and application of serum starvation. *Mashhad Univ. Med. Sci.* **2**, 147–150 (2014).
20. Kim, H. H. *et al.* Nuclear HuR accumulation through phosphorylation by Cdk1. *Genes Dev.* **22**, 1804–15 (2008).